

Nuclear Quantum Effects in liquid water at near classical computational cost using the adaptive Quantum Thermal Bath

Nastasia Mauger^{#,1}, Thomas Plé^{#,2}, Louis Lagardère^{*,1}, Sara Bonella,³
 Étienne Mangaud,² Jean-Philip Piquemal^{*,1} and Simon Huppert^{*2}

¹*Sorbonne Université, LCT, UMR 7616 CNRS, F-75005, Paris, France*

²*CNRS, Sorbonne Université, Institut des NanoSciences de Paris,
 UMR 7588, 4 Place Jussieu, F-75005 Paris, France*

³*CECAM Centre Européen de Calcul Atomique et Moléculaire,*

École Polytechnique Fédérale de Lausanne, Batochimie, Avenue Forel 2, 1015 Lausanne, Switzerland

[#] *These authors contributed equally to this work*

(Dated: December 23, 2024)

We demonstrate the accuracy and efficiency of a recently introduced approach to account for nuclear quantum effects (NQE) in molecular simulations: the adaptive Quantum Thermal Bath (adQTB). In this method, zero point energy is introduced through a generalized Langevin thermostat designed to precisely enforce the quantum fluctuation-dissipation theorem. We propose a refined adQTB algorithm with improved accuracy and we report adQTB simulations of liquid water. Through extensive comparison with reference path integral calculations, we demonstrate that it provides excellent accuracy for a broad range of structural and thermodynamic observables as well as infrared vibrational spectra. The adQTB has a computational cost comparable to classical molecular dynamics, enabling simulations of up to millions of degrees of freedom.

Nuclear quantum effects play a major role in a wide range of physical and chemical processes where light atoms, and especially hydrogen, are involved[1–4]. In particular, a few cutting-edge studies point to their importance in biological systems[5–7], where hydrogen-bonding is ubiquitous, but realistic atomic-scale simulations in that area remain scarce. For such large and complex systems, the most common approach has been to include NQEs implicitly, by fitting analytical potential energy surface models in order to recover experimental thermodynamic properties when performing molecular dynamics (MD) simulations with classical nuclei[8, 9]. However, this strategy potentially limits transferability and its ability to make predictions outside the fitting data set is questionable. Furthermore, the recent developments of new generation polarizable force fields[8, 10–13] and machine learning (ML) potentials[8, 14–17] have opened new perspectives for atomistic simulations of condensed matter systems. These approaches enable high fidelity modeling of the Born-Oppenheimer (BO) energy surface, and can reproduce advanced quantum chemical calculations at only a fraction of their computational cost. Several studies have pointed out that, when reaching such precision on the BO energy, it becomes crucial to account for NQEs explicitly in order to accurately reproduce experimental observation and fully take advantage of the high accuracy achieved[18–21].

Up to now, the conceptual and computational complexity of the simulation methods that allow to account for NQEs explicitly has hindered their spread to a broad community. Reliable results can be obtained in the imaginary-time path integrals (PI) framework [22, 23], by simulating multiple classical replicas of the system (also called beads). This approach provides a numeri-

cally exact reference for static thermodynamic properties (different approximations have also been derived for dynamical observables, as discussed below), but its numerical cost increases linearly with the number of replicas and can become very large compared to classical MD. Several solutions have been proposed to mitigate this cost, such as multiple time stepping in real and imaginary time[24–27] (also known as ring-polymer contraction). This approach, however, is based on a decomposition of the BO energy as a sum of cheap high-frequency and expensive low-frequency terms. Such decomposition is not always feasible and, in particular, it is not easily compatible with the use of machine learning BO energy surfaces. Other developments, such as high-order PI schemes[28, 29], PI perturbation theory[30] or their combination[31] have allowed to efficiently decrease the number of necessary replicas, and reduce the numerical cost associated with PI simulations. The computational overhead still remains important in comparison to classical molecular dynamics (MD) - typically increasing the simulation load by an order of magnitude for hydrogen-bonded systems at room temperature.

A decade ago, a different approach was introduced for the explicit treatment of NQEs with the Quantum Thermal Bath (QTB) [32, 33] and the closely related quantum thermostat[34, 35]. These methods rely on generalized Langevin thermostats in order to approximate the zero-point motion of the nuclei. Although elegant and inexpensive, these methods are only approximate and, in particular, they suffer from zero-point energy (ZPE) leakage from high to low frequency modes which can lead to massive errors in the simulation results[36, 37]. One possible workaround is to combine the generalized thermostat approach with path integrals[38, 39], in order to re-

cover the systematic convergence of PI for large numbers of beads. Even though the number of required replicas is reduced with respect to standard PIMD simulations, the computational cost remains significantly higher than that of classical MD (at least 6 beads are needed for water at ambient conditions[40]). In this letter, we focus on an alternative approach, the adaptive QTB (adQTB) that completely avoids resorting to multiple replicas. In adQTB, the ZPE leakage is compensated directly, using a quantitative criterion derived from the fluctuation-dissipation theorem (FDT). In a previous work[41], the method was successfully tested on model systems, but until now, its applicability to more realistic problems remained to be demonstrated. In the following, we report the main theoretical aspects of the QTB and adQTB methodologies and we introduce two refinements of the adQTB algorithm, that improve its efficiency and accuracy and broaden the range of its possible applications, in particular by enabling reliable constant pressure simulations. We then apply the method to the simulation of liquid water. By careful comparison with path integral references for a wide range of physical properties (structural and thermodynamic properties as well as infrared absorption spectra), we show that, contrary to standard QTB which is plagued by massive ZPE leakage, adQTB is able to capture NQEs with a remarkable accuracy, while its computational overhead remains limited to less than 25% compared to classical MD, allowing to scale up the sample size to over a million atoms.

In QTB and adQTB simulations, each nuclear degree of freedom follows a Langevin-type equation [32]:

$$m_i \frac{d^2 r_i}{dt^2}(t) = -\frac{\partial V}{\partial r_i} - m_i \gamma \frac{dr_i}{dt}(t) + R_i(t) \quad i = 1, \dots, 3N \quad (1)$$

where $V(r_1, \dots, r_i, \dots, r_{3N})$ is the interatomic potential, and m_i is the mass (to simplify notations, the index i denotes both the atom number and the direction x , y or z). The second term on the right-hand side of (1) corresponds to a friction force characterized by the friction coefficient γ . This dissipative term is balanced by the random force $R_i(t)$ that injects energy in the system. In a classical Langevin dynamics, $R_i(t)$ is a white noise, whose amplitude is proportional to temperature. In the QTB, the random force is colored and its correlation spectrum is given by:

$$C_{R_i R_j}(\omega) = 2m_i \gamma_i(\omega) \theta(\omega, T) \delta_i^j \quad (2)$$

where $\gamma_i(\omega)$ is the random force amplitude coefficient, which is simply equal to γ in the standard QTB method, whereas it is adapted on the fly in adQTB (see below). The quantum energy distribution $\theta(\omega, T)$ reads:

$$\theta(\omega, T) = \hbar \omega \left[\frac{1}{2} + \frac{1}{e^{\hbar \omega / k_B T} - 1} \right] \quad (3)$$

It corresponds to the average thermal energy in a quantum harmonic oscillator at frequency ω and temperature

T . Therefore, the aim of the QTB method is to account for ZPE contributions in an otherwise classical dynamics by thermalizing each vibrational mode of the system with an effective energy $\theta(\omega, T)$ instead of the classical thermal energy $k_B T$. However, equations (1-3) by themselves are not sufficient: in the original formulation of the QTB (where the random force amplitude is chosen as $\gamma_i(\omega) = \gamma, \forall \omega$), the ZPE provided to high-frequency modes tends to flow towards low frequencies, which leads to an incorrect energy distribution and can dramatically alter the results. In the adQTB method, this ZPE leakage is quantified precisely using a general result of linear response theory: the quantum fluctuation-dissipation theorem (FDT)[42]. For each degree of freedom i , we define the deviation from the FDT as:

$$\Delta_{FDT,i}(\omega) = \text{Re}[C_{v_i R_i}(\omega)] - m_i \gamma_i(\omega) C_{v_i v_i}(\omega) \quad (4)$$

On the right hand side, $v_i = \frac{dr_i}{dt}$ denotes the velocity, while $C_{v_i v_i}(\omega)$ and $C_{v_i R_i}(\omega)$ are respectively its auto-correlation spectrum and its cross-correlation spectrum with the random force R_i . The FDT characterizes the frequency-dependent distribution of energy in a quantum system at thermal equilibrium. It implies that $\Delta_{FDT,i}(\omega)$ should be zero for any ω , a condition violated in standard QTB simulations, due to ZPE leakage. In adQTB, $\Delta_{FDT,i}(\omega)$ is estimated at regular intervals and the coefficients $\gamma_i(\omega)$ are adjusted via a first-order dynamics to correct for this violation: a negative $\Delta_{FDT,i}(\omega)$ reveals an excess of energy at frequency ω so $\gamma_i(\omega)$ is reduced, and conversely for positive deviations. The adQTB results are produced once the $\gamma_i(\omega)$ have been adapted and $\Delta_{FDT,i}(\omega)$ vanishes (on average, as it is still subject to statistical fluctuations).

In this work, we introduce two refinements with respect to Ref. 41, both of which are presented in full detail in Supplementary Materials. First, to improve the adaptation efficiency, the coefficients $\gamma_i(\omega)$ are adjusted according to the mean FDT deviation, averaged over all equivalent degrees of freedom (i.e. over the 3 directions and over all same-type atoms). Second, we account for the fact that, due to the spectral broadening induced by the friction force, the QTB (and adQTB) tends to slightly underestimate the average potential energy and to overestimate the kinetic energy. This error (unrelated to ZPE leakage) can be predicted and quantified precisely for a harmonic oscillator[43, 44]. In this work, we make use of this harmonic reference and of the deconvolution procedure described in Ref. 45 in order to correct for this inaccuracy. To that end, we slightly modify the random force memory kernel $\theta(\omega, T)$ to compensate for the effect of γ on the potential energy, while the kinetic energy is corrected a posteriori. The kinetic energy correction is significant (more than 10%) and it is essential to enable reliable constant pressure simulations, as its neglect would result in large errors on the pressure estimation (see below and Supplementary Material).

Liquid water is an essential testcase, where the role of NQEs has been extensively investigated in experimental and theoretical studies, and the results of molecular simulations with quantum nuclei have been confronted to experimental data, such as X-ray and neutron diffraction or Compton scattering[46–50]. Water also represents a major challenge for the adQTB, as massive ZPE leakage takes place from the high-frequency intramolecular vibrations (O-H stretching and H-O-H bending modes) toward the slow intermolecular motion[36, 51]. Moreover, net NQEs in water are relatively weak due to the competition between two different quantum contributions[40, 52]: the stretching ZPE (associated with a delocalization of the proton parallel to the O-H direction) tends to strengthen hydrogen bonding between molecules, while the bending ZPE (perpendicular delocalization) tends to weaken it. As a result, NQEs on the structural properties of liquid water are limited[40, 52]. The ability of the adQTB method to capture this subtle balance of NQEs is therefore an important indication of its robustness and it opens new perspectives for its broader application.

In the following, interatomic interactions are modeled by the q-TIP4P/F potential [53] which is widely used as an inexpensive yet realistic benchmark for NQE simulations. This potential was included in a local version of the Tinker-HP massively parallel package[54], in which we also implemented PIMD and (ad)QTB. Periodic boundary conditions were used and electrostatic interactions were computed with the Particle Mesh Ewald method[55]. The calculations are performed with 1000 water molecules (the scalability of the algorithm for larger systems is assessed below). PIMD simulations are converged with 32 beads and require short time steps to ensure accurate integration of the motion. Here we used a 0.2 fs time step for all methods and we checked that increasing it to 1 fs had only a limited effect on the accuracy of the adQTB results, similarly to classical MD (see Supplementary Materials). In classical Langevin MD and PIMD simulations, static averages are independent of the value of the friction parameter γ , and we used $\gamma = 1 \text{ ps}^{-1}$ in both cases, in order to limit the effect of the thermostat on dynamical properties. In the PI case, γ is used for the centroid variables, while the other normal modes are integrated with the optimal friction coefficient of the Thermostated ring-polymer molecular dynamics (TRPMD) scheme[56]. The adQTB, on the other hand, requires relatively large friction coefficients γ , to prevent vanishing of $\gamma_i(\omega)$ during adaptation, which results in incorrect compensation of the ZPE leakage[41]. For liquid water, we estimate that γ should be at least 10 ps^{-1} , but apart from this restriction, we show in Supplementary Materials that the results do not depend significantly on the value of the friction parameter. In the following, we use $\gamma = 20 \text{ ps}^{-1}$ for all QTB and adQTB simulations.

The top panels of Figure 1 show the adapted coupling coefficients obtained in adQTB simulations at 300 K

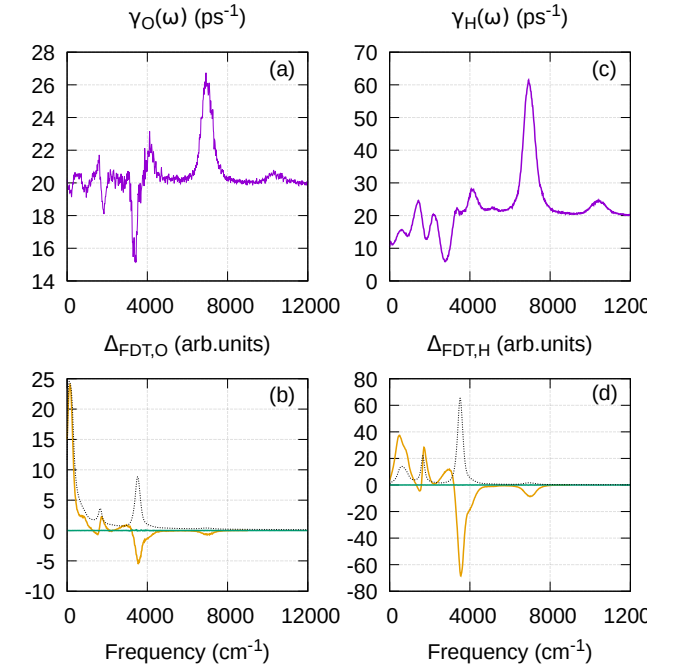


FIG. 1: Panels (a) and (c) show the adapted value of $\gamma_O(\omega)$ and $\gamma_H(\omega)$ for oxygen and hydrogen atoms, respectively (in ps^{-1}). The bottom panel (b) and (d) are the corresponding $\Delta_{FDT}(\omega)$ (in arbitrary units) using the QTB (orange) and adQTB methods (green). The simulations were performed at 300 K and at a fixed volume corresponding to a density $\rho = 0.995 \text{ g.cm}^{-3}$. The average power spectrum $C_{vv}(\omega)$ is represented as a dashed line (in arbitrary units) to facilitate interpretation (see text).

and at constant volume corresponding to a density $\rho = 0.995 \text{ g.cm}^{-3}$. Coefficients for both atom types $\gamma_O(\omega)$ and $\gamma_H(\omega)$ display a similar behavior but with more marked variations in the hydrogen case. As expected, $\gamma_H(\omega)$ is significantly reduced at low frequencies (below 1000 cm^{-1} , corresponding mostly to intermolecular motions) in order to compensate for the energy excess caused by ZPE leakage. The coefficient $\gamma_H(\omega)$ increases around the stretching frequency $\omega_{str} \simeq 3300 \text{ cm}^{-1}$ while $\gamma_O(\omega)$ surprisingly shows a slight decrease. Both coefficients present a sharp peak at the stretching overtone frequency $\omega \simeq 2\omega_{str}$ (a similar but smaller peak is observed at $3\omega_{str}$). In the intermediate frequency range and close to the molecular bending frequency, the coupling coefficients present an intricate oscillation pattern as a function of ω . All these features are robust with respect to changes of the simulation parameters and allow to efficiently compensate for the ZPE leakage, as illustrated by the bottom panels of Fig. 1. They show that the significant deviation $\Delta_{FDT}(\omega)$ from the quantum FDT ob-

served in a standard QTB simulation is practically suppressed in adQTB.

In Figure 2, the QTB (dashed green curve) and adQTB (dashed dotted orange) Radial Distribution Functions (RDFs) are compared with their classical and PIMD counterparts. The most salient NQE for this observable is the strong broadening of the intramolecular peaks in the O-H and H-H RDFs due to the large ZPE contributions of the bending and stretching modes. This effect is very well captured by the adQTB simulations, while it is a little underestimated by the standard QTB due to ZPE leakage. In the O-H RDFs, a very small shift ($\simeq 0.02 \text{ \AA}$) can be seen between the maximum of the PIMD curve and that of the QTB and adQTB curves. This slight inaccuracy of the QTB approach when describing the average distribution of a Morse oscillator (such as the O-H bond in the q-TIP4P/F potential) was already pointed out[44], it is not related to ZPE leakage and therefore not corrected by the adaptation procedure, but it is essentially negligible for water at ambient conditions.

Apart from the notable broadening of the intramolecular distributions, the classical and quantum RDFs are very similar, due to the aforementioned competition of NQEs. In standard QTB simulations, the leakage of the intramolecular ZPE destabilizes the hydrogen bond network completely and all the RDF intermolecular peaks are excessively broadened. On the other hand, Fig. 2 shows that the adQTB procedure efficiently suppresses the leakage so that the corresponding curves are almost superimposed with the PIMD reference (with only very slightly broader features in the adQTB case).

This analysis is further confirmed by Table I, that reports the averages of the different energy terms in the q-TIP4P/F potential. The intermolecular interaction terms (labeled Coulomb and VdW) are only slightly affected by NQEs and their classical and PIMD values are relatively close. In standard QTB simulations, on the other hand, the total intermolecular energy (the sum of the two terms) is overestimated by more than 1 kcal.mol⁻¹ due to ZPE leakage, but this error is well corrected by the adQTB procedure, that recovers intermolecular energy averages very close to the PIMD reference. The adQTB is also remarkably accurate in its estimation of the intramolecular energy terms (labeled AB and BS for angle bending and bond stretching[53]) and of the kinetic energy, that comprise large amounts of ZPE. The method also captures the slight elongation of the OH distance induced by NQEs, while the molecular angle is essentially unaffected. We also computed the dielectric constant and the value obtained from the adQTB simulations at 300 K is 57, in good agreement with our PIMD estimation of 58 as well as that of Ref. 53 (these values are obtained in 12 ns simulations at constant pressure $P = 1 \text{ atm}$ but they are still affected by a statistical uncertainty of a few units).

Although PIMD provides a numerically exact reference

for static quantum properties, the computation of dynamical observables, such as infrared absorption spectra (IRS), represents a much steeper theoretical challenge that is a subject of intense research[56–62]. There is no reference method to compute IRS exactly while accounting for NQEs in complex multiaatomic systems, but a variety of approximate methods has been developed[63–66]. In a recent study, Benson et al. compared different state-of-the-art approximate methods for IRS calculation in liquid water and ice[67]. The authors provide convincing evidence that, within their broad set of approaches, the Linearized semiclassical initial value representation (LSC-IVR) method[65] - where time-correlation functions are computed from short classical trajectories initialized from an approximate sampling of the Wigner distribution - provides the best description of the IRS, while the PI-based thermostated ring-polymer MD (TRPMD)[56] is presented as the cheapest available approach to yield reliable results. QTB has formerly been used with some success as an empirical method to compute approximate IRS[33, 68]. Although not formally derivable from first principles (apart from the trivial harmonic oscillator case), the use of QTB and adQTB for IRS calculations can be justified qualitatively by noting that in QTB simulations, the short-time dynamics is only little affected by the thermostat and is thus essentially classical. Therefore, much like LSC-IVR, the QTB combines classical dynamics with approximate quantum initial value sampling. Furthermore, the deconvolution procedure of Ref. 45 allows to efficiently eliminate the main effect of the QTB thermostat on the (short-time) dynamics, namely the broadening of the spectral peaks due to the friction force.

Fig. 3 compares the IRS computed from adQTB simulations to that obtained in classical MD and TRPMD (for these two cases, a mild Langevin thermostat with $\gamma = 1 \text{ ps}^{-1}$ was used but our results closely agree with the non-thermostated IRS of Ref. 67). Compared to TRPMD, we observe that the low-frequency absorption band computed with adQTB is slightly more intense, and the bending peak (around 1500 cm^{-1}) is a little blue-shifted and broadened. The OH stretching peak at 3500 cm^{-1} is sharper in adQTB than in TRPMD and its overtone at 7000 cm^{-1} has a much larger intensity. These two discrepancies are in favor of the adQTB approach since TRPMD has been shown to cause a spurious broadening of the spectral features and to strongly underestimate anharmonic resonances[67]. Overall, the adQTB IRS are very similar to the LSC-IVR results reported in Ref. 67. This observation should be further confirmed by studies on different systems but it is extremely promising since the computational cost of adQTB is comparable to that of classical MD.

The dynamical properties related to slow molecular motions, on the other hand, cannot be quantitatively assessed in our present adQTB implementation, due to the

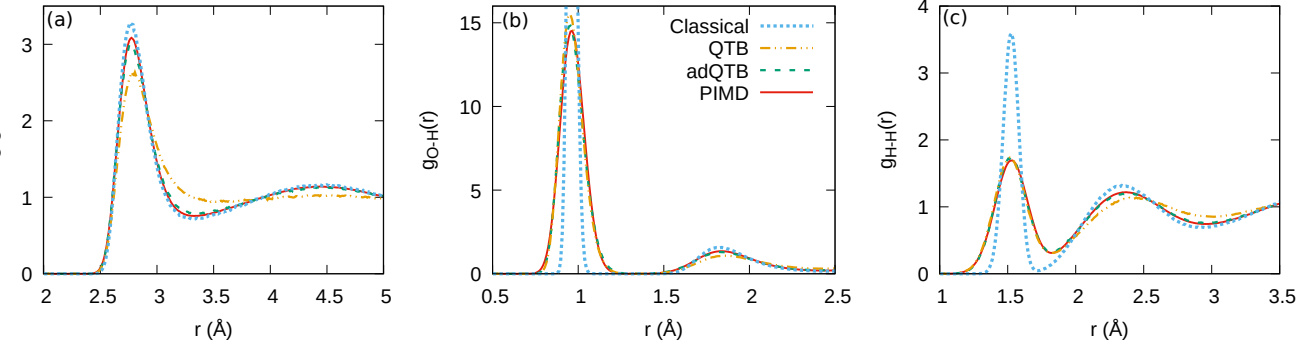


FIG. 2: Radial distribution functions obtained from classical, QTB, adQTB and PIMD simulations at 300K and constant volume corresponding to the density $\rho = 0.995 \text{ g.cm}^{-3}$.

	E_k	E_p	AB	BS	VdW	Coulomb	$r_{OH}[\text{\AA}]$	$\theta_{HOH}(\text{deg})$	$D[10^5 \text{cm}^2 \text{s}^{-1}]$
Classical	2.69	-10.22	0.41	1.18	2.20	-14.00	0.96	104.8	1.89
QTB	8.39	-3.63	1.23	5.81	1.72	-12.38	0.98	104.6	1.65
adQTB	8.60	-4.11	1.17	6.37	2.11	-13.76	0.98	104.7	0.81
PIMD	8.41	-4.29	1.17	6.26	2.15	-13.87	0.98	104.9	2.25

TABLE I: Physical observables obtained with the different methods at 300 K. E_k and E_p denote the kinetic and the total potential energy, while AB, BS and VdW and Coulomb refer to the different energy terms in the q-TIP4P/F potential [53], respectively for molecular Angular Bending, Bond Stretching, Van der Waals interaction and direct Coulomb interaction. All energies are given in kcal.mol^{-1} per water molecule and obtained from 1 ns simulations (preceded by 1.5 ns adaptation for the adQTB) at constant volume corresponding to the density $\rho = 0.995 \text{ g.cm}^{-3}$. The standard errors on the energy values are all inferior to $0.01 \text{ kcal.mol}^{-1}$ per molecule. The table also shows the averages of the oxygen-hydrogen distance r_{OH} and of the molecular angle θ_{HOH} , as well as the self-diffusion coefficient D , that are computed from longer (12 ns) simulations at constant pressure $P = 1 \text{ atm}$. The friction coefficient γ is 20 ps^{-1} in QTB and adQTB, and 1 ps^{-1} in classical MD and PIMD simulations.

need for a relatively large friction coefficient. As shown in Table I, for $\gamma = 20 \text{ ps}^{-1}$, the diffusion coefficient D is underestimated by a factor 2.5 with respect to its RPMD value (a similar decrease of D to 0.75 is observed in classical Langevin simulations with the same γ). The deconvolution procedure used for the IRS is of no use here, since D is related to the zero-frequency component of the vibrational spectrum, and the deconvolution does not provide reliable results in that spectral region[45]. Improved diffusion estimates might still be obtained in future works by decreasing γ selectively at low frequencies using a generalized friction force, or by appropriately redesigning the adQTB algorithm, for example using the recently introduced fast-forward Langevin method[69].

In view of the remarkable performance of the adQTB method for structural and spectral properties, we explored its use to perform fixed pressure simulations using a Langevin piston barostat[70, 71]. Pressure is a challenging quantity to evaluate in the (ad)QTB framework: its estimator is obtained as the difference between two large terms (a potential and a kinetic term, of the order of 10^5 atm each), that almost cancel each other. Therefore,

small inaccuracies on either of these contributions can result in non-negligible errors (see Supplementary materials for more detailed analysis). The results obtained for the density as a function of temperature at $P = 1 \text{ atm}$ are shown in Figure 4.

Because of the competition between NQEs, the classical and PIMD results are very similar, both showing a characteristic bell shape with a maximum around 280 K. NQEs are only responsible for a slight decrease of the density in the intermediate temperature range (270-330 K). The standard QTB method completely fails to capture the temperature-dependence of the density, due to the massive ZPE leakage. It displays a monotonously decreasing trend and strongly overestimates the variations over the temperature range. Compensating the leakage in adQTB allows recovering the overall bell shape and a good agreement with the PIMD reference. In the intermediate temperature range (most relevant for biological systems), the adQTB predictions are very accurate. The curvature of the density curve is only slightly underestimated, leading to small errors of the order of 0.005 g.cm^{-3} in the low-temperature and in the high-

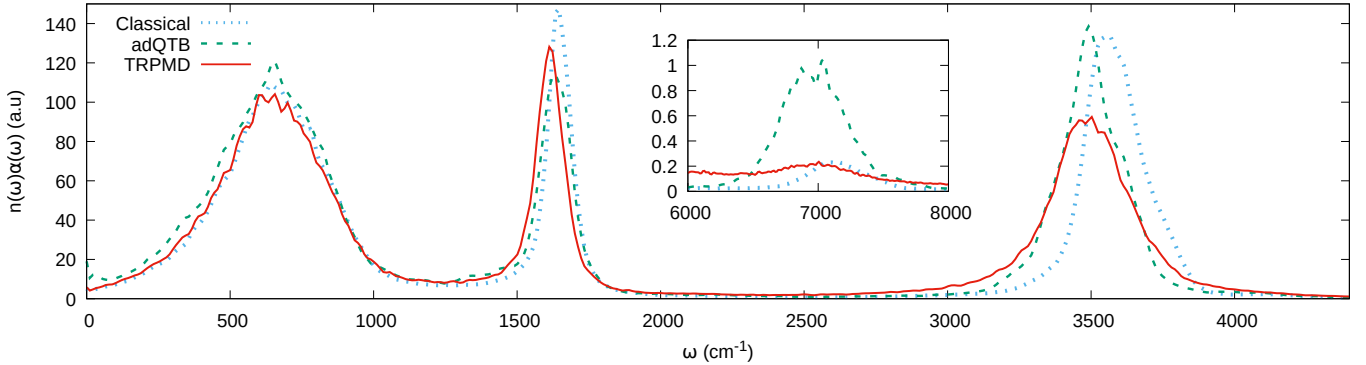


FIG. 3: Infrared absorption spectrum of water at 300 K, given by the product $n(\omega)\alpha(\omega)$ of the refractive index and the absorption coefficient (in arbitrary units). The inset zooms on the peak at the high frequency region. The spectra were deconvoluted from the effect of the thermostat using the procedure of Ref. 45.

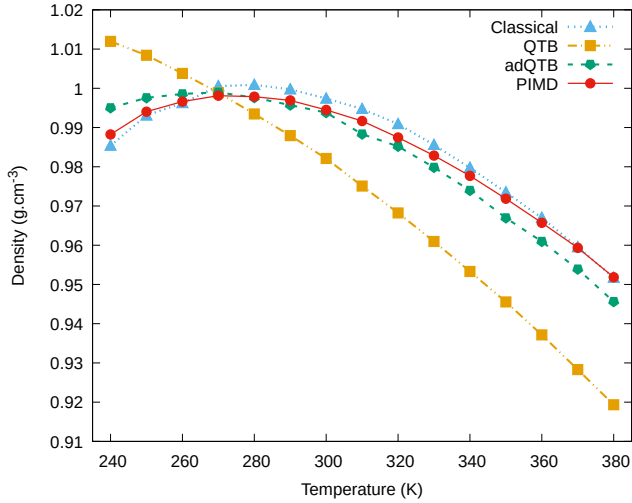


FIG. 4: Density of liquid water at $P = 1$ atm as a function of the temperature.

temperature limits.

These results are encouraging and show that adQTB can be a useful and inexpensive tool to perform NPT simulations of relevant physical and chemical properties that are not critically dependent on the density (Fig. 4 shows that it should still be considered with some caution if high accuracy is required on the density evaluation). As a further illustration, we present on Fig. 5 the enthalpy of vaporization ΔH_{vap} computed in the same NPT simulations as Fig. 4. It has been shown that the NQE play an important role for this observable and need to be included in the simulation for accurate predictions[12, 72]. It is defined as:

$$\Delta H_{vap} = U_g - U_l + P(V_g - V_l) \quad (5)$$

where U_g and U_l are the internal energies in the gas and liquid phases and V_g and V_l are the corresponding av-

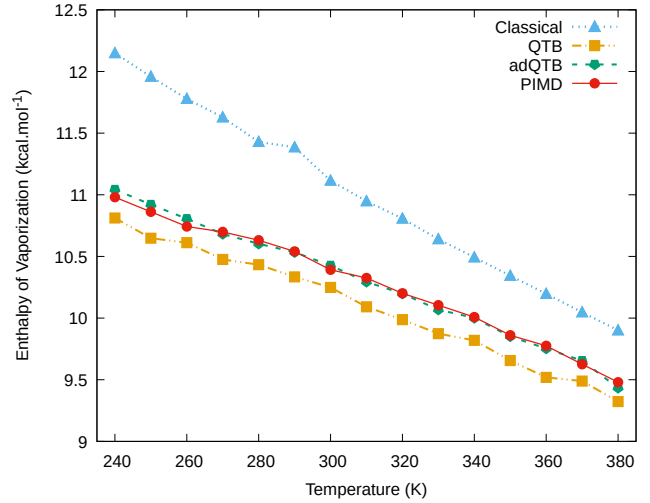


FIG. 5: Enthalpy of vaporization as a function of the temperature.

erage volumes at pressure P . In classical simulations, ΔH_{vap} is systematically overestimated with respect to the corresponding PIMD values. When NQE are included with the standard QTB method, ΔH_{vap} decreases markedly, and becomes even underestimated compared to the PIMD reference. But this discrepancy is in fact due to ZPE leakage and the adQTB allows recovering an almost perfect agreement with the reference, showing that the results are essentially unaffected by the inaccuracies in the determination of the density in the low- and high-temperature ranges.

Finally, we estimate the computational overhead of the adQTB simulations with respect to classical Langevin MD. A first additional cost comes from the generation of the colored random forces, the evaluation of $\Delta_{FDT,i}(\omega)$ and the adaptation of the $\gamma_i(\omega)$ coefficients. This direct cost represents approximately 20% of the total simula-

tion time in the adQTB calculations presented in this study. and in the scalability tests provided in Supplementary Materials, we show that, even for sample sizes over one million atoms, it remains inferior to 25% in our present adQTB implementation - that will be further accelerated using Graphics Processing Units (GPUs)[73]. Furthermore, the q-TIP4P/F water model is particularly inexpensive, and we expect the direct overhead to become negligible in comparison to the atomic force calculations when using more realistic models such as polarizable force fields and ML neural networks. A second source of additional cost stems from the fact that the adaptation procedure requires time for the $\gamma_i(\omega)$ to converge. The necessary adaptation time can vary from one system to the other. In the case of our liquid water simulations, we show in the Supplementary Materials that with an appropriate choice of adaptation parameters, the $\gamma_i(\omega)$ coefficients can converge in about 10 ps. The minimum adaptation time is thus small compared with the several ns of simulation required to reach statistical convergence on some of the physical observables presented in this work, as the density and the dielectric constant.

The adQTB renews the original promise of the QTB method to provide approximate quantum simulations at an almost classical cost, but with a much improved reliability. Our results establish it as a promising alternative to PI methods for an explicit treatment of NQEs in the calculation of static physical properties as well as vibrational spectra. Combined with accurate ML potentials or polarizable force fields, it should provide a powerful tool for a broad range of applications, in particular to the large-scale simulations required in the field of biophysics and biochemistry.

ACKNOWLEDGEMENTS

This work was made possible thanks to funding from the European Research Council (ERC) under the European Union's Horizon 2020 research and innovation program (grant agreement No 810367), project EMC2. Computations have been performed at CINES on the Occigen machine on grant no A0070707671. The authors are grateful to Fabio Finocchi and Philippe Depondt for many interesting discussions.

* louis.lagardere@sorbonne-universite.fr,

* jean-philip.piquemal@sorbonne-universite.fr,

* simon.huppert@sorbonne-universite.fr

- [3] M. Rossi, P. Gasparotto, and M. Ceriotti, *Phys. Rev. Lett.* **117**, 115702 (2016).
- [4] L. Monacelli, I. Errea, M. Calandra, and F. Mauri, *Nature Physics* , 1 (2020).
- [5] P. K. Agarwal, S. R. Billeter, P. R. Rajagopalan, S. J. Benkovic, and S. Hammes-Schiffer, *Proc. Natl. Acad. Sci. USA* **99**, 2794 (2002).
- [6] A. Pérez, M. E. Tuckerman, H. P. Hjalmarson, and O. A. Von Lilienfeld, *Journal of the American Chemical Society* **132**, 11510 (2010).
- [7] L. Wang, S. D. Fried, S. G. Boxer, and T. E. Markland, *Proc. Natl. Acad. Sci. USA* **111**, 18454 (2014).
- [8] G. A. Cisneros, K. T. Wikfeldt, L. Ojamäe, J. Lu, Y. Xu, H. Torabifard, A. P. Bartók, G. Csányi, V. Molinero, and F. Paesani, *Chemical Reviews* **116**, 7501 (2016).
- [9] A. V. Onufriev and S. Izadi, *WIREs Computational Molecular Science* **8**, e1347 (2018).
- [10] C. Liu, J.-P. Piquemal, and P. Ren, *Journal of Chemical Theory and Computation* **15**, 4122 (2019).
- [11] C. Liu, J.-P. Piquemal, and P. Ren, *The Journal of Physical Chemistry Letters* **11**, 419 (2020).
- [12] S. K. Reddy, S. C. Straight, P. Bajaj, C. Huy Pham, M. Riera, D. R. Moberg, M. A. Morales, C. Knight, A. W. Götz, and F. Paesani, *J. Chem. Phys.* **145**, 194504 (2016).
- [13] J. Melcr and J.-P. Piquemal, *Front. Mol. Biosci.* **6**, 143 (2019).
- [14] T. Morawietz and J. Behler, *The Journal of Physical Chemistry A* **117**, 7356 (2013).
- [15] L. Zhang, J. Han, H. Wang, R. Car, and W. E, *Phys. Rev. Lett.* **120**, 143001 (2018).
- [16] J. S. Smith, O. Isayev, and A. E. Roitberg, *Chemical Science* **8**, 3192 (2017).
- [17] A. Singraber, J. Behler, and C. Dellago, *Journal of Chemical Theory and Computation* **15**, 1827 (2019).
- [18] G. S. Fanourgakis and S. S. Xantheas, *J. Chem. Phys.* **128**, 074506 (2008).
- [19] F. Paesani, S. Yoo, H. J. Bakker, and S. S. Xantheas, *The Journal of Physical Chemistry Letters* **1**, 2316 (2010).
- [20] L. Pereyaslavets, I. Kurnikov, G. Kamath, O. Butin, A. Illarionov, I. Leontyev, M. Olevanov, M. Levitt, R. D. Kornberg, and B. Fain, *PNAS* **115**, 8878 (2018).
- [21] B. Cheng, E. A. Engel, J. Behler, C. Dellago, and M. Ceriotti, *Proceedings of the National Academy of Sciences* **116**, 1110 (2019).
- [22] R. P. Feynman, A. R. Hibbs, and D. F. Styer, *Quantum mechanics and path integrals* (Courier Corporation, 2010).
- [23] D. Chandler and P. G. Wolynes, *J. Chem. Phys.* **74**, 4078 (1981).
- [24] T. E. Markland and D. E. Manolopoulos, *J. Chem. Phys.* **129**, 024105 (2008).
- [25] X. Cheng, J. D. Herr, and R. P. Steele, *J. Chem. Th. Comput.* **12**, 1627 (2016).
- [26] V. Kapil, J. VandeVondele, and M. Ceriotti, *J. Chem. Phys.* **144**, 054111 (2016).
- [27] O. Marsalek and T. E. Markland, *J. Chem. Phys.* **144**, 054112 (2016).
- [28] A. Pérez and M. E. Tuckerman, *J. Chem. Phys.* **135**, 064104 (2011).
- [29] V. Kapil, J. Behler, and M. Ceriotti, *J. Chem. Phys.* **145**, 234103 (2016).
- [30] I. Poltavsky and A. Tkatchenko, *Chem. Sci.* **7**, 1368 (2016).

[1] M. Benoit, D. Marx, and M. Parrinello, *Nature* **392**, 258 (1998).

[2] S. Miura, M. E. Tuckerman, and M. L. Klein, *J. Chem. Phys.* **109**, 5290 (1998).

[31] I. Poltavsky, V. Kapil, M. Ceriotti, K. S. Kim, and A. Tkatchenko, *J. Chem. Th. Comput.* **16**, 1128 (2020).

[32] H. Dammak, Y. Chalopin, M. Laroche, M. Hayoun, and J.-J. Greffet, *Phys. Rev. Lett.* **103**, 190601 (2009).

[33] Y. Bronstein, P. Depondt, F. Finocchi, and A. M. Saitta, *Phys. Rev. B* **89**, 214101 (2014).

[34] M. Ceriotti, G. Bussi, and M. Parrinello, *Phys. Rev. Lett.* **103**, 030603 (2009).

[35] M. Ceriotti, G. Bussi, and M. Parrinello, *J. Chem. Theory Comput.* **6**, 1170 (2010).

[36] J. Hernández-Rojas, F. Calvo, and E. G. Noya, *J. Chem. Theory Comput.* **11**, 861 (2015).

[37] F. Brieuc, Y. Bronstein, H. Dammak, P. Depondt, F. Finocchi, and M. Hayoun, *J. Chem. Theory Comput.* **12**, 5688 (2016).

[38] F. Brieuc, H. Dammak, and M. Hayoun, *J. Chem. Theory Comput.* **12**, 1351 (2016).

[39] M. Ceriotti, D. E. Manolopoulos, and M. Parrinello, *J. Chem. Phys.* **134**, 084104 (2011).

[40] M. Ceriotti, W. Fang, P. G. Kusalik, R. H. McKenzie, A. Michaelides, M. A. Morales, and T. E. Markland, *Chemical Reviews* **116**, 7529 (2016).

[41] E. Mangaud, S. Huppert, T. Plé, P. Depondt, S. Bonella, and F. Finocchi, *J. Chem. Theory Comput.* **15**, 2863 (2019).

[42] R. Kubo, *Rep. Prog. Phys.* **29**, 255 (1966).

[43] J.-L. Barrat and D. Rodney, *J. Stat. Phys.* **144**, 679 (2011).

[44] M. Basire, D. Borgis, and R. Vuilleumier, *Phys. Chem. Chem. Phys.* **15**, 12591 (2013).

[45] M. Rossi, V. Kapil, and M. Ceriotti, *J. Chem. Phys.* **148**, 102301 (2018), <https://doi.org/10.1063/1.4990536>.

[46] J. A. Morrone and R. Car, *Phys. Rev. Lett.* **101**, 017801 (2008).

[47] F. Paesani and G. A. Voth, *The Journal of Physical Chemistry B* **113**, 5702 (2009), pMID: 19385690, <https://doi.org/10.1021/jp810590c>.

[48] G. Reiter, J. C. Li, J. Mayers, T. Abdul-Redah, and P. Platzman, *Brazilian Journal of Physics* **34**, 142 (2004).

[49] G. Hura, J. M. Sorenson, R. M. Glaeser, and T. Head-Gordon, *J. Chem. Phys.* **113**, 9140 (2000), <https://doi.org/10.1063/1.1319614>.

[50] G. Romanelli, M. Ceriotti, D. E. Manolopoulos, C. Pantalei, R. Senesi, and C. Andreani, *The Journal of Physical Chemistry Letters* **4**, 3251 (2013).

[51] S. Habershon and D. E. Manolopoulos, *J. Chem. Phys.* **131**, 244518 (2009).

[52] X.-Z. Li, B. Walker, and A. Michaelides, *Proc. Natl. Acad. Sci. USA* **108**, 6369 (2011).

[53] S. Habershon, T. E. Markland, and D. E. Manolopoulos, *J. Chem. Phys.* **131**, 024501 (2009).

[54] L. Lagardère, L.-H. Jolly, F. Lipparini, F. Aviat, B. Stamm, Z. F. Jing, M. Harger, H. Torabifard, G. A. Cisneros, M. J. Schnieders, N. Gresh, Y. Maday, P. Y. Ren, J. W. Ponder, and J.-P. Piquemal, *Chem. Sci.* **9**, 956 (2018).

[55] U. Essmann, L. Perera, M. L. Berkowitz, T. Darden, H. Lee, and L. G. Pedersen, *The Journal of Chemical Physics* **103**, 8577 (1995), <https://doi.org/10.1063/1.470117>.

[56] M. Rossi, M. Ceriotti, and D. E. Manolopoulos, *J. Chem. Phys.* **140**, 234116 (2014).

[57] T. J. Hele, M. J. Willatt, A. Muolo, and S. C. Althorpe, *J. Chem. Phys.* **142**, 134103 (2015).

[58] J. Beutier, R. Vuilleumier, S. Bonella, and G. Ciccotti, *Mol. Phys.* **113**, 2894 (2015).

[59] M. Ceotto, G. Di Liberto, and R. Conte, *Phys. Rev. Lett.* **119**, 010401 (2017).

[60] M. Basire, F. Mouhat, G. Fraux, A. Bordage, J.-L. Haze-mann, M. Louvel, R. Spezia, S. Bonella, and R. Vuilleumier, *J. Chem. Phys.* **146**, 134102 (2017).

[61] G. Trenins, M. J. Willatt, and S. C. Althorpe, *J. Chem. Phys.* **151**, 054109 (2019).

[62] T. Plé, S. Huppert, F. Finocchi, P. Depondt, and S. Bonella, *J. Chem. Phys.* **151**, 114114 (2019), <https://doi.org/10.1063/1.5099246>.

[63] J. Cao and G. A. Voth, *J. Chem. Phys.* **99**, 10070 (1993).

[64] J. Cao and G. A. Voth, *J. Chem. Phys.* **100**, 5093 (1994).

[65] W. H. Miller, *The Journal of Physical Chemistry A* **105**, 2942 (2001).

[66] I. R. Craig and D. E. Manolopoulos, *J. Chem. Phys.* **121**, 3368 (2004).

[67] R. L. Benson, G. Trenins, and S. C. Althorpe, *Faraday Discussions* **221**, 350 (2019).

[68] Y. Bronstein, P. Depondt, L. E. Bove, R. Gaal, A. M. Saitta, and F. Finocchi, *Phys. Rev. B* **93**, 024104 (2016).

[69] M. Hijazi, D. M. Wilkins, and M. Ceriotti, *J. Chem. Phys.* **148**, 184109 (2018), <https://doi.org/10.1063/1.5029833>.

[70] S. E. Feller, Y. Zhang, R. W. Pastor, and B. R. Brooks, *J. Chem. Phys.* **103**, 4613 (1995).

[71] M. Ceriotti, J. More, and D. E. Manolopoulos, *Computer Physics Communications* **185**, 1019 (2014).

[72] B. Guillot and Y. Guissani, *J. Chem. Phys.* **108**, 10162 (1998).

[73] O. Adjoua, L. Lagardère, L.-H. Jolly, A. Durocher, T. Very, I. Dupays, Z. Wang, T. J. Inizan, F. Célerse, P. Ren, J. W. Ponder, and J.-P. Piquemal, “Tinker-hp : Accelerating molecular dynamics simulations of large complex systems with advanced point dipole polarizable force fields using gpus and multi-gpus systems,” (2021), arXiv:2011.01207 [physics.comp-ph].